Supporting Information

Fera et al. 10.1073/pnas.1409954111

SI Methods

Compliance. All work related to human subjects complied with protocols approved by the Duke University Health System Institutional Review Board.

Expression and Purification of Fabs. The heavy- and light-chain variable and constant domains of the unmutated common ancestor (UCA), I3.2, I3.1, and I2 Fabs from the CH103 lineage were cloned into the pVRC-8400 expression vector using Not1 and Nhe1 restriction sites and the tissue plasminogen activator signal sequence. The C terminus of the heavy-chain constructs contained a noncleavable 6x histidine tag. Fabs were expressed using transient transfection of 293T cells using linear polyethylenimine (PEI) following the manufacturer's suggested protocol. After 5 d of expression, supernatants were clarified by centrifugation. His-tagged Fabs were loaded onto Ni-NTA superflow resin (Qiagen) preequilibrated with Buffer A (10mM Tris, pH 7.5, 100 mM NaCl), washed with Buffer A + 10 mM imidazole, and eluted with Buffer A + 350 mM imidazole. Fabs were then purified by gel filtration chromatography in Buffer A using a superdex 200 analytical column (GE Healthcare).

Plasmids containing the CMVR VRC01 Ig heavy and light chains were obtained from the NIH Aids Reagents Program. The protein was expressed in 293F cells as described for Fabs above. The clarified supernatant was diluted twofold using 1x PBS buffer and purified using protein A agarose resin (Pierce), according to manufacturer's protocols. Fractions containing the protein of interest were pooled, concentrated, and further purified by gel filtration chromatography in Buffer A using a superdex 200 analytical column (GE Healthcare). The VRC01 Fab was obtained by digesting the Ig using papain (Pierce) and by running the digested products through protein A resin (Pierce) according to manufacturer's protocol. The Fab was then purified by gel filtration chromatography in Buffer A using a superdex 200 analytical column (GE Healthcare).

Expression and Purification of HIV 92UG037.8 HIV-1 Subtype A Glycoproteins. The IRES-puro vector containing 92UG037.8 HIV-1 subtype A gp120 amino acid (a.a.) residues 1–492 (HXB2 numbering) ΔV123 (core) with a 6x-histidine tag inserted between residues 40 and 41 was kindly provided by Bing Chen (Boston Children's Hospital, Boston, MA). Site-directed mutagenesis was performed using manufacturer's protocols (Stratagene) for D-loop mutants of the CH505 gp120 core and for the V5 mutant of the 92UG037.8 gp120 core. Recombinant Env glycoproteins were expressed in 293T cells and purified as described for His-tagged Fabs.

Design, Expression, and Purification of pVRC8400-HIV-1 Clade C CH505 gp120 ΔV123 Constructs. The codon-optimized synthetic construct of the CH505 T/F HIV-1 subtype C gp120 containing a.a. 41–492 (HXB2 numbering) ΔV123 (core) was produced by GenScript with an N-terminal 6x-histidine tag and inserted into the pVRC-8400 expression vector as described for Fabs. The expression construct contained a leader sequence encoding the tissue plasminogen activator signal sequence

MDAMKRGLCCVLLLCGAVFVSPS

followed by a 6x-histidine tag and the codon-optimized sequence

^{41}GVPVWKEAKTTLFCASDAKAYEKEVHNVWATHACVPTDPNPQEMVLKNVTENFNMWKNDMVDQMHEDVISLWDQSLKPCVKLTPLCVGAGNCNTSVITQACPKVSFDPIPIHYCAPAGYAILKCNNKTFTGTGPCNNVSTVQCTHGIKPVVSTQLLLNGSLAEGEIIIRSENITNNVKTIIVHLNESVKIECTRPGAGYCNINESKWNETLQRVSKKLKEYFPHKNITFQPSSGGDLEITTHSFNCGGEFFYCNTSSLFNRTYMANSTDMANSTETNSTRTITIHCRIKQIINMWQEVGRAMYAPPIAGNITCISNITGLLLTRDGGKNNTETFRPGGGNMKDNWRSELYKYKVVEVK^{492}

between the 5′ NheI and 3′ NotI sites or by the codon-optimized sequence

^{41}GVPVWKEAKTTLFCASDAKAYEKEVHNVWATHACVPTDPNPQEMVLKNVTENFNMWKNDMVDQMHEDVISLWDQSLKPCVKLTPLCVGAGNCNTSVITQACPKVSFDPIPIHYCAPAGYAILKCNNKTFTGTGPCNNVSTVQCTHGIKPVVSTQLLLNGSLAEGEIIIRSENITNNVKTIIVHLNESVKIECTRPGAGYCNINESKWNETLQRVSKKLKEYFPHKNITFQPSSGGDLEITTHSFNCGGEFFYCNTSSLFNRTYMANSTDMANSTETNSTRTITIHCRIKQIINMWQEVGRAMYAPPIAGNITCISNITGLLLTRDGGKNNTDTETFRPGGGNMKDNWRSELYKYKVVEVK^{492}

between the 5′ NheI and 3′ NotI sites for the HIV-1 clade C CH505 gp120 ΔV123 expression construct with a V5 loop DT insertion or by the codon-optimized sequence

^{41}GVPVWKEAKTTLFCASDAKAYEKEVHNVWATHACVPTDPNPQEMVLKNVTENFNMWKNDMVDQMHEDVISLWDQSLKPCVKLTPLCVGAGNCNTSVITQACPKVSFDPIPIHYCAPAGYAILKCNNKTFTGTGPCNNVSTVQCTHGIKPVVSTQLLLNGSLAEGEIIIRSENITNNVKTIIVHLNESVKIECTRPGAGYCNINESKWNETLQRVSKKLKEYFPHKNITFQPSSGGDLEITTHSFNCGGEFFYCNTSSLFNRTYMANSTDMANSTETNSTRTITIHCRIKQIINMWQEVGRAMYAPPIAGNITCISNITGLLLTRDGGKNNTETFETFRPGGGNMKDNWRSELYKYKVVEVK^{492}

between the 5′ NheI and 3′ NotI sites for the HIV-1 clade C CH505 gp120 ΔV123 expression construct with a V5 loop ETF insertion or by the codon-optimized sequence

^{41}GVPVWKEAKTTLFCASDAKAYEKEVHNVWATHACVPTDPNPQEMVLKNVTENFNMWKNDMVDQMHEDVISLWDQSLKPCVKLTPLCVGAGNCNTSVITQACPKVSFDPIPIHYCAPAGYAILKCNNKTFTGTGPCNNVSTVQCTHGIKPVVSTQLLLNGSLAEGEIIIRSENITNNVKTIIVHLNESVKIECTRPGAGYCNINESKWNETLQRVSKKLKEYFPHKNITFQPSSGGDLEITTHSFNCGGEFFYCNTSSLFNRTYMANSTDMANSTETNSTRTITIHCRIKQIINMWQEVGRAMYAPPIAGNITCISNITGLLLTRDGGKNNTEGKNNETFRPGGGNMKDNWRSELYKYKVVEVK^{492}

between the 5′ NheI and 3′ NotI sites for the HIV-1 clade C CH505 gp120 ΔV123 expression construct with a V5 loop EGKNN insertion.

The insert was synthesized (GenScript) to replace the sequence encoding

^{128}TLNCTNATASNSSIIEGMKNCSFNITTELRDKREKKNALFYKLDIVQLDGNSSQYRLI^{194}

from the V1/V2 loop with a sequence encoding a GAG and to replace the sequence encoding

^{300}NNKTRTSIRIGPGQAFYATGQVIGDIREA^{329}

from the V3 loop with a sequence encoding GAG.

Recombinant Env glycoproteins were expressed in 293T cells and purified as described for His-tagged Fabs.

Crystallization. All His-tagged Fabs were crystallized at ~10–12 mg/mL. Crystals were grown in 96-well format using hanging drop vapor diffusion and appeared after 24–48 h at 20 °C. UCA Fab crystals were obtained using microbatch seeding in a condition of 100 mM Hepes, pH 7.0, and 3 M NaCl from seeds of crystals obtained in a condition of 100 mM sodium acetate, pH 4.0, and 2 M ammonium sulfate. I3.2 crystals were grown over a reservoir of 100 mM Hepes, pH 7.0, 2 M ammonium sulfate, and 5% PEG 400; I3.1 crystals were grown over 100 mM sodium acetate, pH 5.0 ,and 2 M ammonium sulfate, and I2 crystals were grown over 100 mM Ches, pH 9.0, 1 M NaCl, and 20% PEG 4K. All crystals were harvested and cryoprotected by the addition of 20–25% glycerol to the reservoir solution and then flash-cooled in liquid nitrogen.

Structure Determination and Refinement. Diffraction data were obtained at 100°K from beam lines 24-ID-E at the Advanced Photon Source and 8.2.2 at the Advanced Light Source using a single wavelength. Datasets from individual crystals (1 crystal for each Fab) were processed with HKL2000 (1). Molecular replacement calculations were carried out with PHASER (2), using CH103 from the CH103/gp120 outer domain complex structure [Protein Data Bank (PDB) ID 4JAN] as the starting model. The CH103 model had to be separated into its variable and constant domains for the UCA and I3.2 Fab structure determinations. There were 4, 2, 4, and 1 molecules per asymmetric unit in the crystals of the UCA, I3.2, I3.1, and I2 Fabs, respectively.

The resulting electron density maps for the UCA and I3.1 were further improved by solvent flattening, histogram matching, and noncrystallographic symmetry averaging using the program DM (3). Phase combination was disabled in these calculations. After density modification, restrained refinement was performed for the UCA and I3.1 Fabs using Refmac in Coot. For all Fabs, subsequent refinement steps were carried out with Refmac (4) and PHENIX (5), and all model modifications were carried out with Coot (6). During refinement, maps were generated from combinations of positional, group B-factor, and TLS (translation/libration/screw) refinement algorithms. Secondary-structure restraints were included at all stages for all Fabs; noncrystallographic symmetry restraints were applied to the UCA and I3.1 Fabs throughout refinement.

The CDRL1 loop, which was three residues longer in all these Fabs than that in the CH103 Fab, was built manually using Coot. The final refined structures contain residues 2–214 (heavy chain) and 2–209 (light chain) for the UCA, residues 1–215 (heavy chain) and 2–209 (light chain) for I3.2, residues 1–215 (heavy chain) and 2–209 (light chain) for I3.1, and residues 2–215 (heavy chain) and 3–209 (light chain) for I2. Density missing elsewhere is discussed in *Results*. Structure validations were performed periodically during refinement for each of the Fabs using the MolProbity server (5). The final refinement statistics are summarized in Table S1. The UCA, I3.2, I3.1, and I2 structures had, respectively, 87.4%, 92.7%, 89.7%, and 90.6% of their residues in favored regions of the Ramachandran plot, and 0.7%, 1.5%, 3.0%, and 2.6% in outlying regions. The Cα rmsd of three of the molecules in the UCA asymmetric unit from the fourth are 0.276 Å, 0.459 Å, and 0.448 Å, and the last two have an rmsd of 0.292 Å relative to each other; the rmsd of the two I3.2 molecules in an asymmetric unit is 0.356 Å; the rmsd of three of the four molecules of I3.1 in an asymmetric unit from the fourth are 0.233 Å, 0.187 Å, and 0.198 Å.

Protein Structure Analysis and Graphical Representations. The heavy chains of the UCA, I3.2, I3.1, and I2 were superposed on that of the CH103 Fab by least squares fitting in Coot. The rmsds of different molecules in the asymmetric unit of a particular Fab were determined using PyMol by superposing the entire Fab molecules. To calculate Cα rmsds between different Fabs, we used only the framework regions of the Fabs, as defined in Chothia et al. (7). All graphical representations with protein crystal structures were made using PyMol.

Biolayer Interferometry Measurements. Kinetic measurements of Fab binding to the autologous CH505 gp120 core and heterologous 92ug037.8 gp120 core and their corresponding mutants were carried out using the Octet QK^e system (ForteBio); 0.2 mg/mL of each His-tagged Fab was immobilized onto an anti-Human Fab-CH1 biosensor until it reached saturation. The gp120 core mutants were tested at concentrations of 1 μM to 36 μM, depending on the mutant. A reference sample of buffer alone was used to account for any signal drift that was observed during the experiment. Association and dissociation were each monitored for 5 min. All experiments were conducted in the Octet instrument at 30 °C in a buffer of 10 mM Tris, pH 7.5, and 100 mM NaCl with agitation at 1,000 rpm. Analyses were performed using a global fit of at least three measurements using nonlinear regression curve fitting using the Graphpad Prism software, version 6.

1. Otwinowski Z, Minor W (1997) *Processing of X-Ray Diffraction Data Collected in Oscillation Mode* (Academic, New York).
2. McCoy AJ (2007) Solving structures of protein complexes by molecular replacement with Phaser. *Acta Crystallogr D Biol Crystallogr* 63(Pt 1):32–41.
3. Cowtan K (1994) "dm": An automated procedure for phase improvement by density modification. *Joint CCP4 and ESF-EACBM Newsletter on Protein Crystallography* 31:34–38.
4. Winn MD, et al. (2011) Overview of the CCP4 suite and current developments. *Acta Crystallogr D Biol Crystallogr* 67(Pt 4):235–242.
5. Adams PD, et al. (2010) PHENIX: A comprehensive Python-based system for macromolecular structure solution. *Acta Crystallogr D Biol Crystallogr* 66(Pt 2):213–221.
6. Emsley P, Cowtan K (2004) Coot: Model-building tools for molecular graphics. *Acta Crystallogr D Biol Crystallogr* 60(Pt 12 Pt 1):2126–2132.
7. Chothia C, Lesk AM (1987) Canonical structures for the hypervariable regions of immunoglobulins. *J Mol Biol* 196(4):901–917.
8. Liao HX, et al.; NISC Comparative Sequencing Program (2013) Co-evolution of a broadly neutralizing HIV-1 antibody and founder virus. *Nature* 496(7446):469–476.

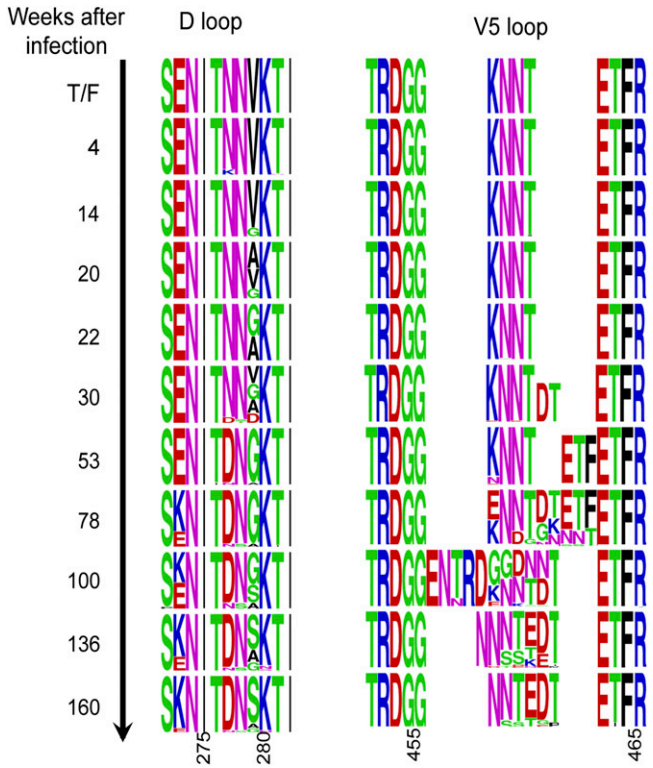

Fig. S1. Sequence logo of the D and V5 loops at the time points indicated on the left. The frequency of each amino acid is shown by its height; spaces allow for deletions and insertions. Amino acid position numbers are based on HIV-1 HXB2 numbering. GSTYC polar residues are green; NQ neutral residues, purple; KRH basic residues, blue; DE acidic residues, red; and PAWFLIMV hydrophobic residues, black.

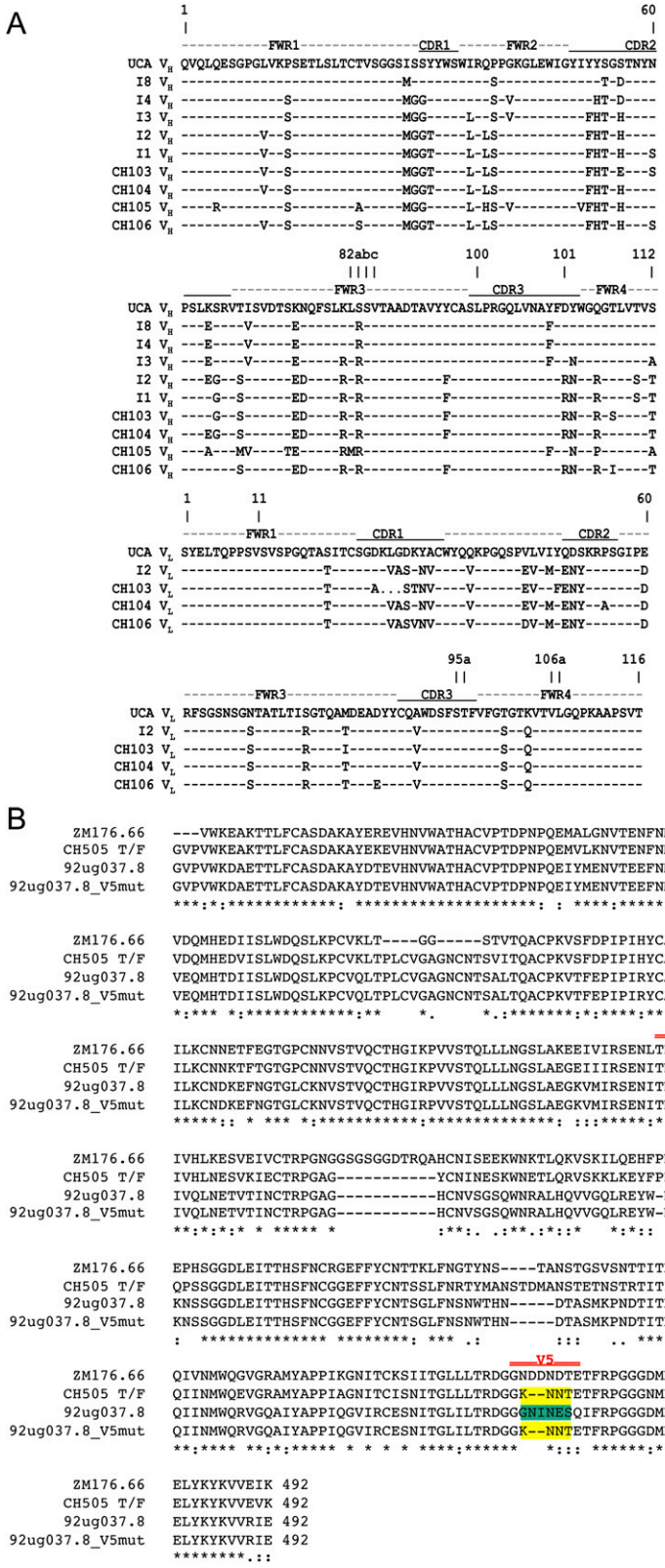

Fig. S2. Sequence alignments. (*A*) CH103 Fab sequences. Alignment of the heavy- and light-chain variable-regions sequences. Complementarity determining region (CDR) loops and the framework region (FR) for each chain are indicated. Conserved residues with respect to the UCA are marked by a dash. (*B*) Alignment of different HIV gp120 core constructs. Conserved residues are indicated by a star (*); conservative substitutions, by a semicolon (:); and substitutions that change the charge, by a period (.) below the alignment. Sequence numbers are based on the HIV-1 HXB2 numbering. The D and V5 loop regions are indicated, with highlights for the most substantial variation.

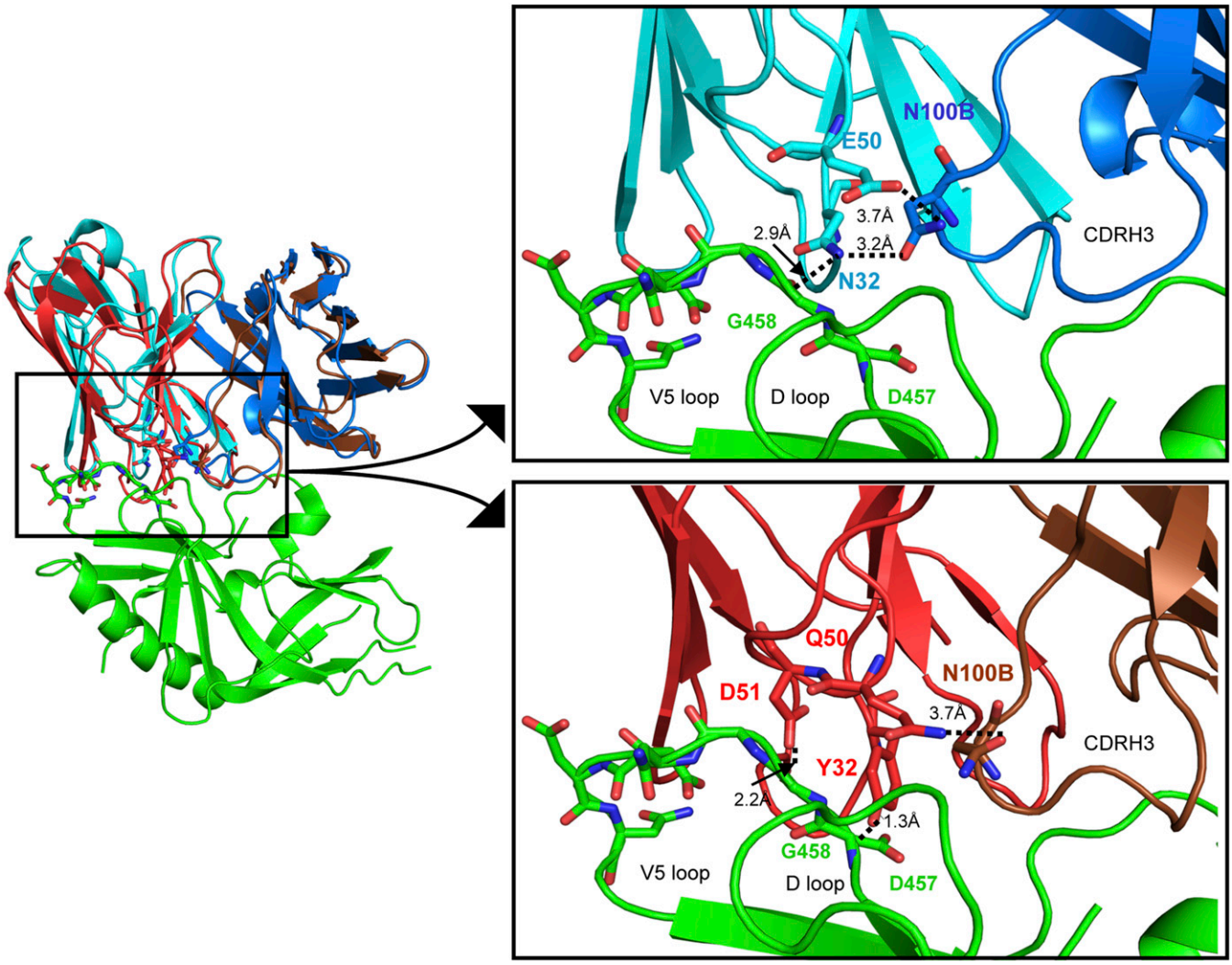

Fig. S3. Superposition of the UCA Fab with the CH103/gp120 outer domain complex. Zoomed images of the light-chain CDR1 and heavy-chain CDR3 regions of CH103 (*Upper*) (light chain in cyan and heavy chain in blue) in complex with ZM176.66 gp120 [in green; PDB ID code 4JAN (8)] and the UCA superposed onto the CH103 Fab as described in the text (*Lower*) (light chain in red and heavy chain in brown); the zoomed images include the V5 and D loops of gp120. Distances in Å show (favorable) hydrogen bonds (*Upper*) and unfavorable contacts (clashes) (*Lower*). Images created in PyMol.

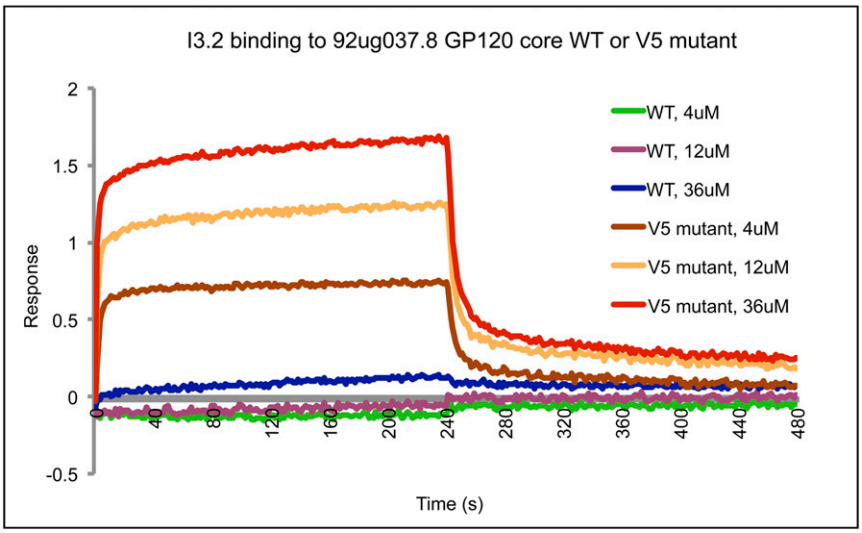

Fig. S4. Representative curves from biolayer interferometry. The Fab was immobilized onto an anti-human Fab-CH1 biosensor, and gp120 constructs were introduced at three or more different concentrations, ranging from low micromolar to midmicromolar, depending on the mutant tested. Fits and affinities derived as described in *SI Methods*.

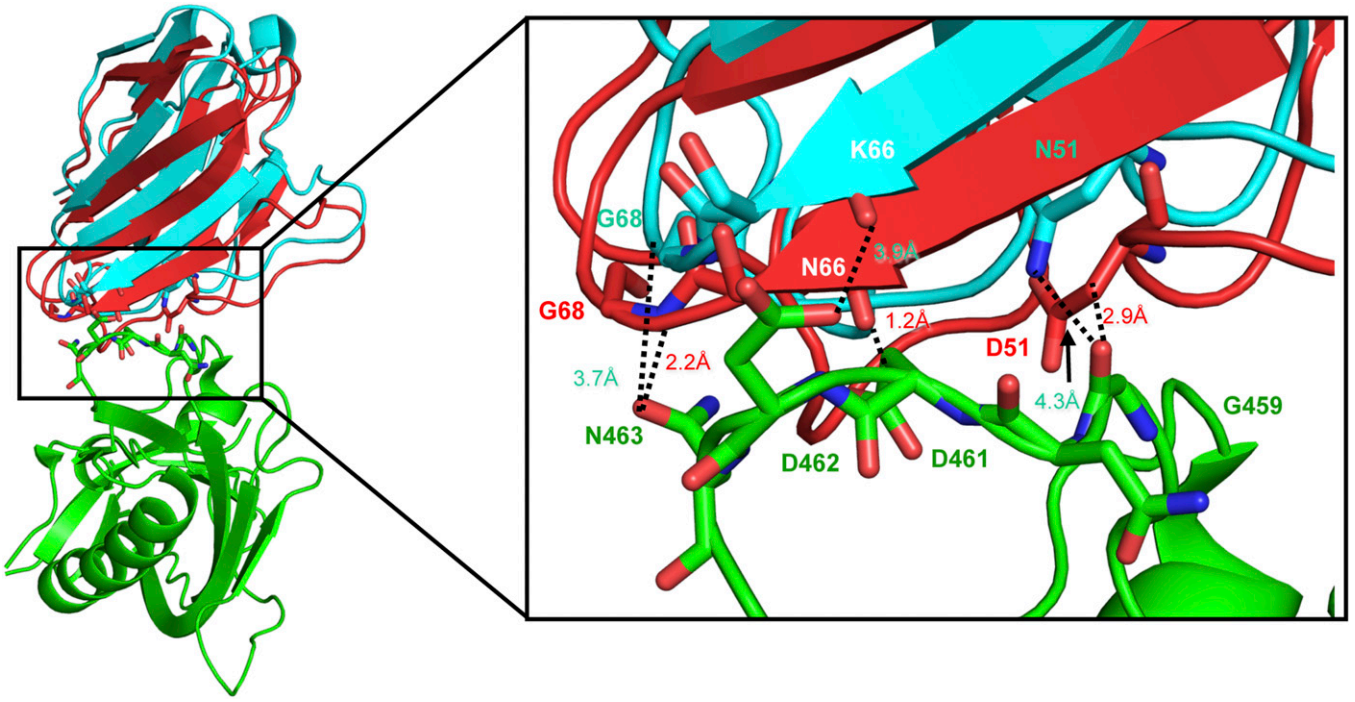

Fig. S5. Superposition of the UCA Fab with the CH103/gp120 outer domain complex. A zoomed in image of the superposed light-chain CDR2 and FR3 regions of the UCA (red) and CH103 (cyan) in complex with gp120; the gp120 V5 loop is shown (green). Amino acids that either clash or hydrogen bond are shown as sticks, along with distances between the V5 loop and CH103 (cyan) or the UCA (red). Images created in PyMol.

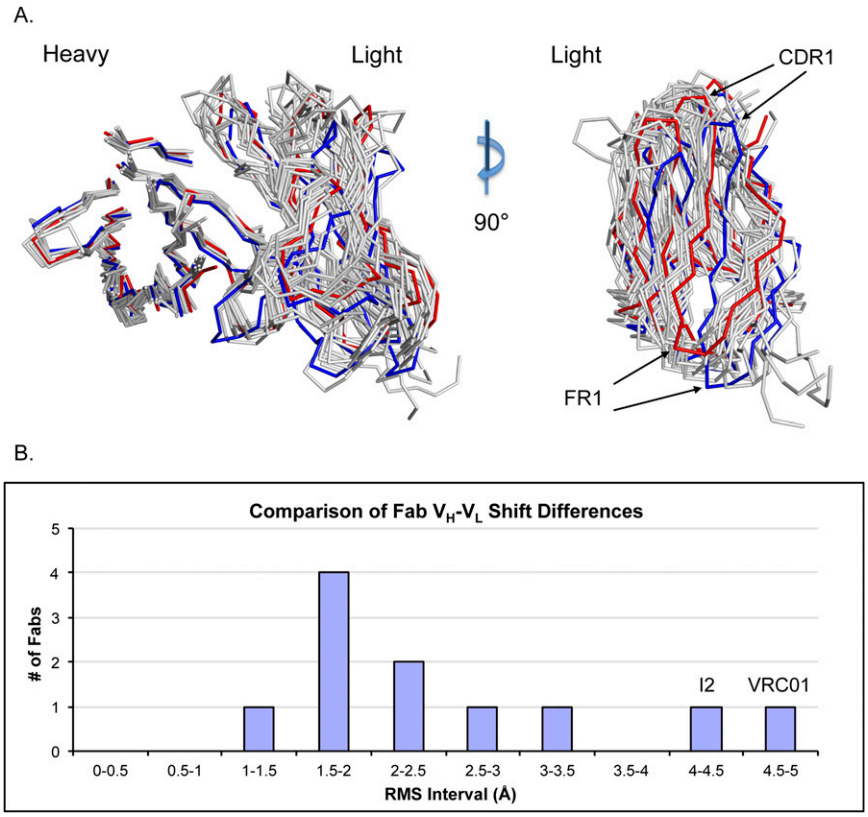

Fig. S6. Superposition of the UCA and I2 Fabs with other human Fabs. (*A*) Overlay of Fab variable domains. Two orthogonal views of Fabs superposed on the V_H framework region of the UCA Fab (red). The I2 Fab (blue) and 10 additional human Fabs (gray) are shown. Heavy chain residues 17–25 and 33–52 (Kabat numbering) were superposed on that of the UCA. Their FR1 and CDR1 regions are marked for reference. Image created in PyMol. (*B*) Distribution of rmsds. The bars indicate how many Fabs have a V_L with the indicated root-mean-squared deviation range with respect to the UCA V_L. The light-chain framework residues included for these calculations are: 3–12, 17–25, 33–52, 56–60, 68–82, 88–95, 102–112 (Kabat numbering). I2 from the CH103 lineage is also included for reference. The rmsd of the VRC01 V_L with respect to the I2 V_L is 2.61 Å.

Table S1. Data collection and refinement statistics

	UCA	I3.2	I3.1	I2
Data collection				
Space group	$P12_11$	$P2_12_12_1$	$P3_112$	$P2_12_12_1$
Cell dimensions				
a, *b*, *c* (Å)	78.7, 71.1, 184.4	72.1, 99.1, 163.3	132.3, 132.3, 209.6	55.9, 67.0, 128.8
α, β, γ (°)	90, 93.8, 90	90, 90, 90	90, 90, 120	90, 90, 90
Resolution (Å)	46.85–3.49 (3.56–3.49)*	49.57–3.15 (3.20–3.15)	48.04–3.23 (3.29–3.23)	46.42–3.00 (3.05–3.00)
R_{sym} or R_{merge}	14.4 (37.3)	12.3 (38.6)	11.4 (65.0)	10.5 (80.6)
$I/\sigma(I)$	7.1 (3.0)	7.7 (2.1)	6.7 (1.1)	9.6 (1.3)
Completeness (%)	96.5 (95.1)	99.0 (98.1)	98.9 (97.6)	97.6 (97.5)
Redundancy	3.0 (3.0)	2.2 (2.2)	1.9 (2.0)	2.3 (2.3)
Refinement				
Resolution (Å)	46.85–3.49	49.57–3.15	48.04–3.23	46.42–3.00
No. reflections	23,779	20,706	33,905	10,152
R_{work}/R_{free} (%)	26.9/ 28.5	23.7/28.2	22.4/25.1	22.6/27.2
No. atoms				
Protein	12,800	6,454	12,840	3,220
Ligand/ion				
Water				
B-factors				
Protein	66.2	59.4	85.5	87.6
Ligand/ion				
Water				
rms deviations				
Bond lengths (Å)	0.005	0.003	0.004	0.004
Bond angles (°)	1.18	0.787	0.978	0.986

*Values in parentheses are for highest-resolution shell. One crystal of each Fab was used for data collection.

Table S2. Cα rmsd (Å) of the framework variable domains of CH103 lineage Fabs

	UCA	I3.2	I3.1	I2	CH103
UCA	0				
I3.2	0.41	0			
I3.1	0.94	1.05	0		
I2	0.92	0.94	0.54	0	
CH103	1.07	1.01	0.73	0.74	0

Table S3. Cα rmsd (Å) of the individual V_H (white) and V_L (gray) framework domains of CH103 lineage Fabs

	UCA	I3.2	I3.1	I2	CH103
UCA	0	0.38	0.43	0.44	0.46
I3.2	0.45	0	0.27	0.33	0.33
I3.1	0.54	0.41	0	0.36	0.34
I2	0.68	0.45	0.45	0	0.42
CH103	0.57	0.38	0.31	0.41	0

Values shaded in gray were determined by comparing the V_L framework domains of the indicated Fabs; values in white regions were determined by comparing V_H framework domains.

Table S4. CH505 gp120 core binding to CH103 Fabs

	UCA			I3.2			I2			VRC01		
CH505 gp120 core	K_d $\times 10^{-6}$ M	k_a $\times 10^{3}$ M^{-1} s^{-1}	k_d $\times 10^{-1}$ s^{-1}	K_d $\times 10^{-6}$ M	k_a $\times 10^{3}$ M^{-1} s^{-1}	k_d $\times 10^{-1}$ s^{-1}	K_d $\times 10^{-6}$ M	k_a $\times 10^{3}$ M^{-1} s^{-1}	k_d $\times 10^{-1}$ s^{-1}	K_d $\times 10^{-6}$ M	k_a $\times 10^{2}$ M^{-1} s^{-1}	k_d $\times 10^{-4}$ s^{-1}
WT	2.40 ± 0.04	87.16 ± 2.84	2.10 ± 0.06	1.36 ± 0.03	61.93 ± 1.60	0.84 ± 0.02	2.19 ± 0.04	46.46 ± 1.17	1.01 ± 0.02	1.16 ± 0.03	11.27 ± 0.21	13.03 ± 0.17
WT, V281G	3.34 ± 0.08	68.25 ± 2.90	2.28 ± 0.09	1.79 ± 0.03	52.97 ± 1.13	0.95 ± 0.02	2.30 ± 0.04	37.44 ± 0.84	0.86 ± 0.01	3.78 ± 0.10	16.68 ± 0.38	63.08 ± 0.97
WT, V281A	2.73 ± 0.08	73.19 ± 3.62	2.00 ± 0.09	1.42 ± 0.03	57.96 ± 1.48	0.82 ± 0.02	1.75 ± 0.04	40.48 ± 1.02	0.71 ± 0.01	1.17 ± 0.03	9.54 ± 0.17	11.20 ± 0.14
WT, N279D	2.86 ± 0.07	80.09 ± 3.80	2.29 ± 0.10	1.58 ± 0.03	54.65 ± 1.32	0.86 ± 0.02	1.79 ± 0.03	52.95 ± 1.33	0.95 ± 0.02	0.78 ± 0.02	11.39 ± 0.23	8.87 ± 0.14
WT, N279D, V281G	2.85 ± 0.08	87.58 ± 4.99	2.50 ± 0.13	1.71 ± 0.04	60.29 ± 1.76	1.03 ± 0.02	1.68 ± 0.04	44.10 ± 1.19	0.74 ± 0.01	1.49 ± 0.03	13.40 ± 0.22	19.93 ± 0.22
DT (V5 insert)	>100	–	–	13.07 ± 0.46	29.11 ± 1.87	3.81 ± 0.21	4.50 ± 0.12	68.35 ± 3.66	3.08 ± 0.15	1.41 ± 0.04	4.32 ± 0.07	6.07 ± 0.11
DT + V281G	10.46 ± 0.61	35.01 ± 3.62	3.66 ± 0.33	16.74 ± 0.45	22.95 ± 1.11	3.84 ± 0.16	4.42 ± 0.10	58.18 ± 2.40	2.57 ± 0.09	2.52 ± 0.05	3.92 ± 0.05	9.89 ± 0.10
DT + V281A	12.95 ± 0.40	35.63 ± 2.21	4.62 ± 0.26	13.12 ± 0.35	34.70 ± 1.84	4.55 ± 0.22	3.71 ± 0.08	55.53 ± 2.00	2.06 ± 0.06	1.47 ± 0.04	4.12 ± 0.07	6.07 ± 0.10
DT + N279D	15.29 ± 0.64	34.96 ± 3.14	5.35 ± 0.44	8.83 ± 0.40	51.39 ± 4.46	4.54 ± 0.35	4.82 ± 0.11	58.61 ± 2.80	2.82 ± 0.12	1.28 ± 0.04	5.44 ± 0.11	6.95 ± 0.14
DT + N279D, V281G	14.14 ± 0.55	37.87 ± 3.17	5.35 ± 0.41	9.41 ± 0.33	49.63 ± 3.36	4.67 ± 0.28	4.87 ± 0.11	40.73 ± 1.63	1.98 ± 0.07	2.02 ± 0.05	2.85 ± 0.04	5.76 ± 0.09
ETF (V5 insert)	NB	–	–	>100	–	–	21.17 ± 0.58	6.24 ± 0.23	1.32 ± 0.04	1.44 ± 0.04	3.98 ± 0.07	5.75 ± 0.11
ETF + V281G	NB	–	–	>100	–	–	11.19 ± 0.26	14.98 ± 0.55	1.68 ± 0.05	2.09 ± 0.06	6.67 ± 0.12	13.9 ± 0.18
ETF + V281A	NB	–	–	>100	–	–	6.01 ± 0.15	20.32 ± 0.76	1.22 ± 0.04	1.00 ± 0.03	4.92 ± 0.09	4.94 ± 0.11
ETF + N279D	NB	–	–	>100	–	–	13.21 ± 0.36	11.70 ± 0.42	1.55 ± 0.04	1.38 ± 0.04	4.61 ± 0.09	6.34 ± 0.12
ETF + N279D, V281G	NB	–	–	>100	–	–	3.28 ± 0.07	45.69 ± 1.32	1.50 ± 0.03	1.32 ± 0.04	5.66 ± 0.10	7.49 ± 0.12
EGKNN (V5 insert)	NB	–	–	>100	–	–	>100	–	–	1.17 ± 0.04	4.51 ± 0.08	5.27 ± 0.10
EGKNN + N279D, V281G	NB	–	–	>100	–	–	5.68 ± 0.16	42.19 ± 1.90	2.40 ± 0.09	1.57 ± 0.05	4.70 ± 0.09	7.39 ± 0.13

Biolayer interferometry data were analyzed as described in *SI Methods*. The averages and SEs are for three runs using different gp120 concentrations. The K_d values are derived by a global fit of all of the data for each experiment. Association rate constant (k_a) and dissociation rate constant and (k_d) are also given. Red indicates no binding; orange indicates equilibrium dissociation constants great than 100 μM; and yellow indicates equilibrium dissociation constants between 10 μM and 100 μM. NB, no binding (detected).